

# $N$ Two-Transmon-Qubit Quantum Logic Gates Realized in a Circuit QED System

T. Said<sup>1,\*</sup>, A. Chouikh<sup>1</sup> and M. Bennai<sup>1,2</sup>

<sup>1</sup> Laboratoire de Physique de la Matière Condensée, Equipe Physique Quantique et Applications, Faculté des Sciences Ben Msik, B.P. 7955, Université Hassan II, Casablanca, Maroc

<sup>2</sup> LPHE-Modélisation et Simulation, Faculté des Sciences Rabat, Université de Rabat, Maroc

Received: 2 Jan. 2019, Revised: 10 Apr. 2019, Accepted: 12 Apr. 2019

Published online: 1 Sep. 2019

**Abstract:** We theoretically present an effective method to realize  $Ni$ SWAP,  $N(\sqrt{i}$ SWAP),  $NSWAP$ ,  $N(\sqrt{SWAP})$  and  $NTQ$ -NOT gates based on the qubit-qubit interaction in a circuit QED using  $N+1$  transmon qubits driven by a strong microwave field. In this system, the interaction between the qubits and the resonator field can be achieved by turning the gate voltage and the external flux. The operation time is independent of the number of qubits involved in the scheme, and the gates operations are insensitive to the initial state of the resonator. These quantum logic gates can be realized in a time (nanosecond-scale) much smaller than decoherence time (microsecond-scale), and it is more immune to the  $1/f$  charge noise and has longer dephasing time due to the favorable properties of the transmon qubits in the circuit QED. Numerical simulation under the influence of the gates operations shows that the scheme can be implemented with high fidelity. We also propose a detailed procedure and experimentally analyze its feasibility. Moreover, the scheme might be experimentally achieved efficiently within current state-of-the-art technology.

**Keywords:** Transmon qubit,  $Ni$ SWAP gate,  $NSWAP$  gate,  $NTQ$ -NOT gate,  $N\sqrt{i}$ SWAP gate,  $N\sqrt{SWAP}$  gate, circuit QED.

## 1 Introduction

Quantum computation has attracted much attention since a quantum computer has an ability to solve hard computational problems with high efficiency compared to a classical computer [1, 2, 3]. Also, it is well known that it is difficult to simulate the behaviour of a quantum mechanical system with a classical computer. The difficulty arises because quantum systems are not confined to their eigenstates but can in general exist in any superposition of them, thus the vector space needed to describe the system is extremely large. Quantum logic gates are the basic building blocks of a quantum computer [4, 5]. A universal quantum computer can be built on a series of two-qubit logic gates [6, 7]. Up to now, a large number of theoretical proposals have been introduced to implement various gates, such as two-qubit Controlled-NOT (CNOT) gate [8], SWAP gate [9],  $i$ SWAP gate [10],  $\sqrt{i}$ SWAP gate [8] and  $\sqrt{SWAP}$  gate [11] in different systems, such as cavity QED system [13] and circuit QED system [14]. The circuit QED is

currently the promising candidate for future quantum computer.

Recently, Yang et al. [15] proposed a novel scheme for implementing multi-qubit quantum controlled-phase gate with one superconducting qubit simultaneously controlling  $n$  qubits selected from  $N$  qubits ( $1 < n < N$ ). In ref. [16] the authors proposed a scheme to realize  $NTCP$  gate in a circuit QED by using the system of  $(N+1)$  transmon qubits. The method of implementing  $n$  qubits SWAP gates simultaneously between one superconducting charge qubit with  $n$  qubits coupled to a cavity was firstly proposed by Song et al. [17].

In recent works, We have proposed another type of multiqubit controlled gate that is a  $NTCP$  gate by using qubit-qubit interaction in a circuit QED [18]. Also, we have presented a method for realizing  $NTCP$ -NOT and  $NTQ$ -NOT gates with one control superconducting qubit simultaneously controlling  $N$  target qubits in a cavity QED [19]. In the present study, we present and demonstrate a method for realizing  $N$  two-transmon-qubit quantum logic gates ( $Ni$ SWAP,  $N\sqrt{i}$ SWAP,  $NSWAP$ ,

\* Corresponding author e-mail: [taoufik.said81@gmail.com](mailto:taoufik.said81@gmail.com)

$N\sqrt{\text{SWAP}}$ , and NTQ-NOT gates) of one transmon qubit simultaneously controlling  $N$  target transmon qubits in circuit QED with nearest qubit-qubit interaction by adding a strong microwave field. These type of quantum logic gates are useful in quantum computation and quantum information processing. On the other hand, the qubit-qubit interaction could influence the evolution of the system used in ref. [17]. Moreover, the presence of both qubit-qubit interaction and Jaynes-Cummings make our system powerful.

The paper is organized as follows: In Sec.2, we concretely illustrate the way  $Ni\text{SWAP}$ ,  $N\sqrt{i\text{SWAP}}$ ,  $N\text{SWAP}$ ,  $N\sqrt{\text{SWAP}}$  and NTQ-NOT gates via circuit QED by using the system of  $N + 1$  transmon qubits coupled to a resonator with nearest qubit-qubit interaction, we have calculated the evolution operator a three-step, we use the overall evolution operator for obtaining these quantum logic gates, we also give a brief discussion about our proposal. In Sec.3, we study the fidelity and then discuss its feasibility based on current experiments in circuit QED. A concluding summary is given in Sec.4.

## 2 Basic theory

The method presented for implementing  $N$  two-transmon-qubit quantum logic gates ( $Ni\text{SWAP}$ ,  $N\sqrt{i\text{SWAP}}$ ,  $N\text{SWAP}$ ,  $N\sqrt{\text{SWAP}}$  and NTQ-NOT gates) via circuit QED is based on the qubit-qubit interaction. In this subsection, we show how to apply the first method to implement these quantum logic gates which the transmon qubits are capacitively coupled to a superconducting transmission line resonator (TLR) driven by a strong microwave field. The physical setup considered in this study is schematically illustrated in Fig.1. The operation time of these gate is shorten because the coupling constant between the transmon qubit and the quantum date bus (QDB) is large enough in the case of TLR has been chosen as QDB. The similar architectures have been used in refs. [20].

Let us now consider an  $(N + 1)$  transmon qubits which are capacitively coupled to a TLR driven by a strong microwave field [20] as depicted in Fig.1. A microwave field of frequency  $\omega_d$  is applied to the input wire of the TLR. The  $(N + 1)$  transmon qubits each having two-level subspaces driven by a conventional field added, these transmon qubits are capacitively coupled to it. Moreover, the qubit-qubit interaction should be included in the circuit QED [21], where the direct interaction between the qubits, in circuit QED, is virtually realized in the dispersive regime [22]. The Hamiltonian of the whole system (assuming  $\hbar = 1$ ) given by [18]

$$H = \omega_q \sum_{j=1}^{N+1} \sigma_{z,j} + \omega_r a^\dagger a + \Omega \sum_{j=1}^{N+1} (\sigma_j^+ e^{-i\omega_d t} + \sigma_j^- e^{i\omega_d t}) + \sum_{j=1}^{N+1} g_j (a^\dagger \sigma_j^- + a \sigma_j^+) + \sum_{j,k=1, j \neq k}^{N+1} \Gamma_{jk} \sigma_j^+ \sigma_k^-, \quad (1)$$

we get  $\Omega = g_j \varepsilon / \delta$  where  $\delta = \omega_r - \omega_d$  is the detuning between the resonance frequency of the TLR  $\omega_r$  and the frequency of the external drive applied to the TLR  $\omega_d$ ,  $\Gamma_{jk} = g_j g_k (\frac{1}{\Delta_j} + \frac{1}{\Delta_k})$  [22] which describes the effective interaction between qubits  $j$  and  $k$ , and  $\Delta_j (\Delta_k)$  is large detuning as compared to the qubit-TLR coupling  $g_j (g_k)$  [23].  $\sigma_{z,j}$ ,  $\sigma_j^-$ , and  $\sigma_j^+$  are the collective operators for the  $(1, 2, \dots, N + 1)$  qubits, which are given by  $\sigma_{z,j} = \frac{1}{2}(|0_j\rangle\langle 0_j| - |1_j\rangle\langle 1_j|)$ ,  $\sigma_j^+ = |1_j\rangle\langle 0_j|$ ,  $\sigma_j^- = |0_j\rangle\langle 1_j|$  where  $|1_j\rangle (|0_j\rangle)$  is the excited state (ground state) of the transmon qubit,  $\omega_r = 1/\sqrt{LC}$  is the resonance frequency of the TLR where the transmission line resonator can be modeled as a simple harmonic oscillator composed of the parallel combination of an inductor  $L$  and a capacitor  $C$ ,  $\omega_q$  is the transition frequency of the transmon qubit with  $\omega_{q1} = \omega_{q2} = \dots = \omega_{qN+1}$ ,  $a^\dagger, a$  are the creation and annihilation of the resonator mode. In the high  $E_J/E_C$  limit the transition frequency between the ground state  $|0_j\rangle$  and excited state  $|1_j\rangle$  is given by  $\omega_q = \sqrt{8E_J E_C}/\hbar$ , where  $E_C = e^2/2C_\Sigma$  and  $E_J(\Phi) = E_{J0} |\cos(\pi\Phi/\Phi_0)|$ ,  $C_\Sigma = C_S + (C_g^{-1} + C_g'^{-1})^{-1}$ . Here,  $C_g, C_g'$  are the gate capacitance,  $C_S$  is the additional capacitor,  $C_\Sigma$  is the effective total capacitance,  $\Phi$  is the external magnetic flux applied to the SQUID loop,  $\Phi_0 = h/2e$  is the flux quantum,  $E_J(\Phi)$  is the effective Josephson coupling energy,  $E_C$  is the charging energy, and  $E_{J0}$  is the Josephson coupling energy, where the qubit work at the regime  $E_J/E_C \gg 1$ . It is obvious that the frequency of the transmon qubit  $\omega_q$  can be tuned by external magnetic flux  $\Phi$ . When we work with a large amplitude driving field, quantum fluctuations in the drive are very small with respect to the drive amplitude and the drive can be considered, for all practical purposes, as a classical field.

For convince, we assume that we can tune the coupling constant  $g_j$  and the coupling strength  $\Gamma_{jk}$  at the same time to have  $g_j = g_k = g$  and  $\Gamma_{jk} = \Gamma = \frac{2g^2}{\Delta}$  (in the case  $\Delta_j = \Delta_k = \Delta$ ). By assuming that  $\omega_d = \omega_q$ , we have the following Hamiltonian  $H_I$  in the interaction picture [18]

$$H_I = \Omega \sum_{j=1}^{N+1} (\sigma_j^+ + \sigma_j^-) + g \sum_{j=1}^{N+1} (e^{i\delta t} a \sigma_j^+ + e^{-i\delta t} a^\dagger \sigma_j^-) + \Gamma \sum_{j,k=1, j \neq k}^{N+1} \sigma_j^+ \sigma_k^-, \quad (2)$$

where  $\delta = \omega_r - \omega_q$  is the detuning between the frequency of the qubit  $\omega_q$  and the frequency of the resonator  $\omega_r$ . When  $\Omega \gg \delta, g, \Gamma$  and  $\delta \gg g, \Gamma$  we can get the Hamiltonian  $H_I$  in the interaction picture [15, 24, 25, 26]

$$H_I = H_0 + H_{eff}, \quad (3)$$

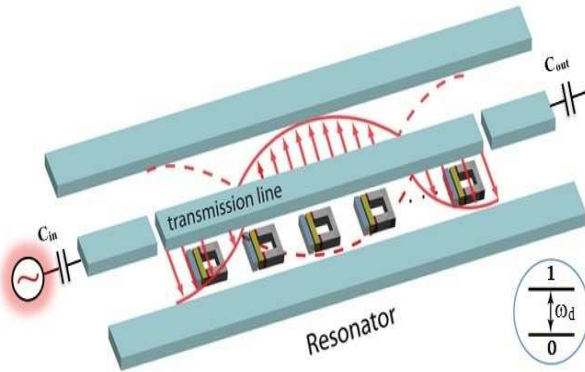


**Fig. 1:** (Color online) Schematic diagram of a TLR and several  $(N + 1)$  transmon qubits are coupled in a circuit QED (blue) driven by a strong microwave field of frequency  $\omega_d$  (this field  $\sim$  is applied to the input wire of the TLR). The TLR is connected to the input wiring with a capacitor  $C_{in}$ , and output wiring with a capacitor  $C_{out}$ . In addition, the coupling between qubits  $i$  and  $j$  is via inductances coupling, where this coupling can be interpreted as an energy coupling between qubits.

with

$$H_0 = 2\Omega \sum_{j=1}^{N+1} \sigma_{x,j} \quad (4)$$

$$H_{eff} = \frac{g^2}{\delta} \left[ \sum_{j=1}^{N+1} (\sigma_j^+ \sigma_j^- + a^+ a \sigma_{z,j}) + \sum_{j,k=1, j \neq k}^{N+1} \sigma_j^+ \sigma_k^- \right] + \Gamma \sum_{j,k=1, j \neq k}^{N+1} \left( \sigma_{x,j} \sigma_{x,k} + \frac{1}{4} (\sigma_j^+ \sigma_k^- + \sigma_j^- \sigma_k^+) \right), \quad (5)$$

where  $\sigma_{x,j} = \frac{1}{2} (\sigma_j^+ + \sigma_j^-)$ . From Eq.3, we can easily

obtain the corresponding evolution operator  $U(t)$  as follows [15, 25, 27]

$$U(t) = \exp \left\{ -i2\Omega t \sum_{j=1}^{N+1} \sigma_{x,j} - i\frac{g^2}{\delta} t \left[ \sum_{j=1}^{N+1} (\sigma_j^+ \sigma_j^- + a^+ a \sigma_{z,j}) + \sum_{j,k=1, j \neq k}^{N+1} \sigma_j^+ \sigma_k^- \right] - i\Gamma t \sum_{j,k=1, j \neq k}^{N+1} \left[ \frac{1}{2} \sigma_{x,j} \sigma_{x,k} + \frac{1}{4} (\sigma_j^+ \sigma_k^- + \sigma_j^- \sigma_k^+) \right] \right\}. \quad (6)$$

For a charge qubit 1 coupled to the resonator, assumed  $\delta \gg |g|$ . Then, the corresponding evolution operator can be expressed as [17, 28]

$$U_{11}(t) = \exp \left[ -2i\Omega t \sigma_{x,1} - i\frac{g^2}{\delta} t (\sigma_1^+ \sigma_1^- + a^+ a \sigma_{z,1}) \right]. \quad (7)$$

We now show how to utilize the above model (Eq.6) to implement an  $Ni$ SWAP,  $N\sqrt{i}$ SWAP,  $NSWAP$ ,  $N\sqrt{S}$ WAP and  $NTQ$ -NOT gates. We note that: (i) for each one of qubits  $1, 2, \dots, N + 1$  of each step of the operations, the dc gate voltage  $V_g^{dc} = e/C_g$ , such that  $E_z = 0$  for each qubit, and (ii) the resonator mode frequency  $\omega_r$  is fixed during the entire operation. We now consider two special cases:  $\delta > 0$  as well as  $\delta < 0$ . The results from the unitary evolution, obtained for these two special cases, are employed below for the gate implementation. The detailed procedure is given as follows:

**Step 1.** Let us begin with the case  $\delta > 0$ , set  $V_g^{ac} = V_0 \cos(\omega t)$  for each qubit, adjust the transition frequencies of  $(N + 1)$  qubits by external flux  $\Phi_j$ , then  $\omega_q = \omega_d$  is satisfied, with the pulse Rabi frequency  $\Omega = g\mathcal{E}/\delta$  of the amplitude  $V_0$  where the detuning  $\delta = \omega_r - \omega_q > 0$ . So, after a period of evolution time  $\tau_1 = 2\pi/\delta$ , the evolution operator for the qubit system corresponding to this step would be the  $U_1(t)$  of Eq.6.

$$U(\tau_1) = \exp \left\{ -i2\Omega \tau \sum_{j=1}^{N+1} \sigma_{x,j} - i\frac{g^2}{\delta} \tau \left[ \sum_{j=1}^{N+1} (\sigma_j^+ \sigma_j^- + a^+ a \sigma_{z,j}) + \sum_{j,k=1, j \neq k}^{N+1} \sigma_j^+ \sigma_k^- \right] - i\Gamma \tau \sum_{j,k=1, j \neq k}^{N+1} \left[ \sigma_{x,j} \sigma_{x,k} + \frac{1}{4} (\sigma_j^+ \sigma_k^- + \sigma_j^- \sigma_k^+) \right] \right\}, \quad (8)$$

**Step 2.** Let us now consider the case  $\delta < 0$ , set  $V_g^{ac} = 0$  for qubit 1, adjust the level spacings of qubit 1 such that the resonator mode is coupled to qubits  $(2, 3, \dots, N + 1)$ , so  $\omega_q = \omega_d$  is satisfied, with the pulse Rabi frequency is  $\Omega'$  of the amplitude  $V_0'$ , where the detuning  $\delta' = \omega_r - \omega_q' = -\delta > 0$ . Then, after a period of time  $\tau_2 = 2\pi/\delta'$ , the evolution operator of the system corresponding to this step can be described by

$$U(\tau_2) = \exp \left\{ -i2\Omega \tau \sum_{j=2}^{N+1} \sigma_{x,j} - i\frac{g^2}{\delta} \tau \left[ \sum_{j=2}^{N+1} (\sigma_j^+ \sigma_j^- + a^+ a \sigma_{z,j}) + \sum_{j,k=2, j \neq k}^{N+1} \sigma_j^+ \sigma_k^- \right] - i\Gamma \tau \sum_{j,k=2, j \neq k}^{N+1} \left[ \sigma_{x,j} \sigma_{x,k} + \frac{1}{4} (\sigma_j^+ \sigma_k^- + \sigma_j^- \sigma_k^+) \right] \right\}, \quad (9)$$

The combined time evolution operator of the whole system, after these two steps, is arrived at

$$U(\tau_1 + \tau_2) = \exp \left\{ -i2\Omega \tau \sigma_{x,1} - i\frac{g^2}{\delta} \tau (\sigma_1^+ \sigma_1^- + a^+ a \sigma_{z,1}) - i\frac{g^2}{\delta} \tau \sum_{j=2}^{N+1} (\sigma_1^+ \sigma_j^- + \sigma_1^- \sigma_j^+) - i\Gamma \tau \sum_{j=2}^{N+1} \left[ \sigma_{x,1} \sigma_{x,j} + \frac{1}{2} (\sigma_1^+ \sigma_j^- + \sigma_1^- \sigma_j^+) \right] \right\}. \quad (10)$$

**Step 3.** We adjust the transition frequency of qubits  $2, 3, \dots, N + 1$  such that the resonator mode is largely

decoupled from each qubit, but we leave the transition frequency unchanged for qubit 1 such that  $g^2/|\delta'| \ll |g|$  (i.e.  $|\delta'| \gg |g|$  where  $\delta' < 0$ ) and  $\Omega' = g\varepsilon/\delta'$ . When the condition  $\delta' = -\delta$  is satisfied, the time evolution operator after a period of time  $\tau$  is [17, 28]

$$U_{I1}(\tau_3) = \exp \left[ 2i\Omega\tau\sigma_{x,1} + i\frac{g^2}{\delta}\tau(\sigma_1^+\sigma_1^- + a^+a\sigma_{z,1}) \right]. \quad (11)$$

After the three-step process, a phase flip (i.e.,  $|1\rangle \rightarrow -|1\rangle$ ) on the state  $|1\rangle$  of each target transmon qubit is achieved when the control transmon qubit 1 is initially in the state  $|1\rangle$ , but nothing happens to the states  $|0\rangle$  and  $|1\rangle$  of each target transmon qubit when the control transmon qubit 1 is initially in the state  $|0\rangle$ . When the conditions  $\frac{\Gamma}{2} + \frac{g^2}{\delta} = \gamma$  and  $\Gamma = 4\chi$ , the evolution operator of the system, after the above three steps operation, is given by

$$U_s(\tau) = \prod_{j=2}^{N+1} U_{gate}(1, j), \quad (12)$$

where

$U_{gate}(1, j) = \exp[-i\chi\tau 4\sigma_{x,1}\sigma_{x,j} - i\gamma\tau(\sigma_1^+\sigma_j^- + \sigma_1^-\sigma_j^+)]$ ,  $j = 2, 3, \dots, N+1$ . In the next section, we will use this evolution operator of the whole system (Eq.12) for demonstrate how  $NiSWAP$ ,  $N\sqrt{iSWAP}$ ,  $NSWAP$ ,  $N\sqrt{SWAP}$  and  $NTQ$ -NOT gates can be realized.

### 3 Preparation of quantum logic gates and discussion

#### 3.1 Implementation of $NiSWAP$ and $N\sqrt{iSWAP}$ gates

It is demonstrated that more complex quantum gates can be created by the  $iSWAP$  and  $\sqrt{iSWAP}$  gates [29]. Furthermore, the  $iSWAP$  and  $\sqrt{iSWAP}$  gates forms a universal gate set, a CNOT gate for example can be obtained from two  $iSWAP$  or two  $\sqrt{iSWAP}$  gates and single-qubit rotations [4]. Recently, it has been shown that the  $iSWAP$  and  $\sqrt{iSWAP}$  gates can be very useful for applications in quantum information process QIP and quantum computing [30]. The purely quantum  $iSWAP$  and  $\sqrt{iSWAP}$  gates are an appropriate elementary two-qubit gates, these quantum logic gates can be represented by the the following input–output operators:

$$iSWAP \equiv |00\rangle\langle 00| + i|01\rangle\langle 10| + i|10\rangle\langle 01| + |11\rangle\langle 11|. \quad (13)$$

$$\sqrt{iSWAP} \equiv \begin{bmatrix} 1 & 0 & 0 & 0 \\ 0 & \frac{1}{\sqrt{2}} & \frac{i}{\sqrt{2}} & 0 \\ 0 & \frac{i}{\sqrt{2}} & \frac{1}{\sqrt{2}} & 0 \\ 0 & 0 & 0 & 1 \end{bmatrix}. \quad (14)$$

The goal of this subsection is to demonstrate how the  $NiSWAP$  and  $N\sqrt{iSWAP}$  gates can be realized based on

the evolution operator of the whole system (Eq.12). According to the evolution operator  $U_{gate}(1, j)$  above (from Eq.12) on the basis  $(|0_1\rangle, |1_1\rangle)$  for qubit 1, so the basis  $(|0_j\rangle, |1_j\rangle)$  for qubit  $(2, 3, \dots, N+1)$ , we can obtain following evolutions

$$\begin{aligned} U_{gate}(1, j)|0_1\rangle|0_j\rangle &= \cos\chi\tau|0_1\rangle|0_j\rangle - i\sin\chi\tau|1_1\rangle|1_j\rangle \\ U_{gate}(1, j)|0_1\rangle|1_j\rangle &= e^{i\eta\pi} [\cos(\gamma+\chi)\tau|0_1\rangle|1_j\rangle \\ &\quad - i\sin(\gamma+\chi)\tau|1_1\rangle|0_j\rangle] \\ U_{gate}(1, j)|1_1\rangle|0_j\rangle &= e^{i\eta\pi} [\cos(\gamma+\chi)\tau|1_1\rangle|0_j\rangle \\ &\quad - i\sin(\gamma+\chi)\tau|0_1\rangle|1_j\rangle] \\ U_{gate}(1, j)|1_1\rangle|1_j\rangle &= \cos\chi\tau|1_1\rangle|1_j\rangle - i\sin\chi\tau|0_1\rangle|0_j\rangle, \end{aligned} \quad (15)$$

A phase factor  $\eta\pi$  in the previous evolutions can be produced by several different proposals [31]. By setting  $\chi\tau = 2k\pi$  (with  $k$  being an integer),  $\eta = 2m$  (with  $m$  being an integer) and  $\gamma\tau = (2n + \frac{3}{2})\pi$  (with  $n$  being an integer), we obtain  $N$ -two-qubit  $iSWAP$  operations as (from Eq.15)

$$\begin{aligned} U_{iSWAP}(1, j)|0_1\rangle|0_j\rangle &= |0_1\rangle|0_j\rangle \\ U_{iSWAP}(1, j)|0_1\rangle|1_j\rangle &= i|1_1\rangle|0_j\rangle \\ U_{iSWAP}(1, j)|1_1\rangle|0_j\rangle &= i|0_1\rangle|1_j\rangle \\ U_{iSWAP}(1, j)|1_1\rangle|1_j\rangle &= |1_1\rangle|1_j\rangle. \end{aligned} \quad (16)$$

By setting  $\chi\tau = 2k\pi$  (with  $k$  being an integer),  $\eta = 2m$  (with  $m$  being an integer) and  $\gamma\tau = (2n + \frac{5}{4})\pi$  (with  $n$  being an integer), we obtain  $N$ -two-qubit  $\sqrt{iSWAP}$  operations as

$$\begin{aligned} U_{\sqrt{iSWAP}}(1, j)|0_1\rangle|0_j\rangle &= |0_1\rangle|0_j\rangle \\ U_{\sqrt{iSWAP}}(1, j)|0_1\rangle|1_j\rangle &= \frac{1}{\sqrt{2}} [|0_1\rangle|1_j\rangle + i|1_1\rangle|0_j\rangle] \\ U_{\sqrt{iSWAP}}(1, j)|1_1\rangle|0_j\rangle &= \frac{1}{\sqrt{2}} [|1_1\rangle|0_j\rangle + i|0_1\rangle|1_j\rangle] \\ U_{\sqrt{iSWAP}}(1, j)|1_1\rangle|1_j\rangle &= |1_1\rangle|1_j\rangle. \end{aligned} \quad (17)$$

Then, the  $N$  two qubit  $iSWAP$  and  $\sqrt{iSWAP}$  operations are simultaneously performed on  $N$  qubit pairs  $(1, 2)$ ,  $(1, 3)$ , ...,  $(1, N+1)$ . Each gate operation ( $iSWAP$  and  $\sqrt{iSWAP}$  gate) includes the same control qubit and a different target qubit. Thus, the  $NiSWAP$  and  $N\sqrt{iSWAP}$  gates are implemented simultaneously between the first qubit and the  $N$  qubits. Finally, we give a brief discussion about our proposal. We notice that  $\delta$  satisfies the equation  $(g/\delta_1)^2 = n + \frac{3}{4}$  of the  $NiSWAP$  gate and the equation  $(g/\delta_2)^2 = n + \frac{5}{8}$  of the  $\sqrt{iSWAP}$  gate, where  $n$  is an integer. So, when  $n = 0$ ,  $\delta$  takes maximum  $\delta_1 = \frac{2\sqrt{3}}{3}g$  and  $\delta_2 = \frac{2\sqrt{10}}{5}g$ . Then, the operation time  $t_{op1} = 3\tau = 2\pi \times \frac{3\sqrt{3}}{2g}$  ( $NiSWAP$  gate) and  $t_{op2} = 3\tau = 2\pi \times \frac{3\sqrt{10}}{4g}$  ( $\sqrt{iSWAP}$  gate) are independent of the number of target qubits  $N$ . Then, the direct

calculation shows that the operations times required to implement the  $Ni$ SWAP and  $\sqrt{i}$ SWAP gates with transmon qubits are  $t_{op1} = 13ns$  and  $t_{op2} = 11.86ns$ . In the next, we use the above evolutions (Eq.15) for implementing NSWAP, NTQ-NOT and  $N\sqrt{SWAP}$  gates.

### 3.2 Implementation of NSWAP and $N\sqrt{SWAP}$ gates

The SWAP and  $\sqrt{SWAP}$  gates are an appropriate elementary two-qubit gates, where they are useful in quantum computation and quantum information processing [4], such as establishing the universality of two-qubit gates [32], programmable gate arrays [33], and constructing quantum circuits [34]. On the other hand, the SWAP gate is equivalent to three CNOT gates and the  $\sqrt{SWAP}$  gate constitutes a universal set of quantum gates together with single qubit rotations around an arbitrary axis [11]. these type of quantum logic gates can be represented by the operators:

$$SWAP \equiv |00\rangle\langle 00| + |01\rangle\langle 10| + |10\rangle\langle 01| + |11\rangle\langle 11| \quad (18)$$

$$\sqrt{SWAP} \equiv \begin{bmatrix} 1 & 0 & 0 & 0 \\ 0 & \frac{1+i}{2} & \frac{1-i}{2} & 0 \\ 0 & \frac{1-i}{2} & \frac{1+i}{2} & 0 \\ 0 & 0 & 0 & 1 \end{bmatrix}. \quad (19)$$

The main objective of this subsection is to realize NSWAP and  $\sqrt{SWAP}$  gates using the evolutions (Eq.15). By selecting  $\chi\tau = 2k\pi$  (with  $k$  being an integer),  $\eta = 2m + \frac{1}{2}$  (with  $m$  being an integer) and  $\gamma\tau = (2n + \frac{1}{2})\pi$  (with  $n$  being an integer), an  $N$  two qubit SWAP operations are simultaneously performed on  $N$  qubit pairs  $(1, 2), (1, 3), \dots, (1, N + 1)$  as (from Eq.15)

$$\begin{aligned} U_{SWAP}(1, j)|0_1\rangle|0_j\rangle &= |0_1\rangle|0_j\rangle \\ U_{SWAP}(1, j)|0_1\rangle|1_j\rangle &= |1_1\rangle|0_j\rangle \\ U_{SWAP}(1, j)|1_1\rangle|0_j\rangle &= |0_1\rangle|1_j\rangle \\ U_{SWAP}(1, j)|1_1\rangle|1_j\rangle &= |1_1\rangle|1_j\rangle. \end{aligned} \quad (20)$$

By setting  $\chi\tau = 2k\pi$  (with  $k$  being an integer),  $\eta = 2m + \frac{1}{4}$  (with  $m$  being an integer) and  $\gamma\tau = (2n + \frac{1}{4})\pi$  (see Eq.15), we obtain  $N$ -two-qubit  $\sqrt{SWAP}$  operations as

$$\begin{aligned} U_{\sqrt{SWAP}}(1, j)|0_1\rangle|0_j\rangle &= |0_1\rangle|0_j\rangle \\ U_{\sqrt{SWAP}}(1, j)|0_1\rangle|1_j\rangle &= \frac{1+i}{2}|0_1\rangle|1_j\rangle + \frac{1-i}{2}|1_1\rangle|0_j\rangle \\ U_{\sqrt{SWAP}}(1, j)|1_1\rangle|0_j\rangle &= \frac{1+i}{2}|1_1\rangle|0_j\rangle + \frac{1-i}{2}|0_1\rangle|1_j\rangle \\ U_{\sqrt{SWAP}}(1, j)|1_1\rangle|1_j\rangle &= |1_1\rangle|1_j\rangle. \end{aligned} \quad (21)$$

By this way, one can see that NSWAP and  $N\sqrt{SWAP}$  gates are simultaneously performed on the qubit pairs  $(1, 2), (1, 3), \dots, (1, N + 1)$ , respectively. So, the NSWAP

and  $N\sqrt{SWAP}$  gates are implemented simultaneously between one transmon qubit and  $N$  transmon qubits. Hence, it is clear that the NSWAP and  $N\sqrt{SWAP}$  gates can be realized after the three-step process. Now, we give a brief discussion about quantum NSWAP and  $N\sqrt{SWAP}$  gates, we notice that  $\delta$  satisfies the equation  $(g/\delta_3)^2 = n + \frac{1}{4}$  of the NSWAP gate and the equation  $(g/\delta)^2 = n + \frac{1}{8}$  of the  $N\sqrt{SWAP}$ , where  $n$  is an integer, when  $n = 0$ ,  $\delta$  takes maximum  $\delta_3 = 2g$  and  $\delta_4 = 2\sqrt{2}g$ . Then, the operations times required to implement the NSWAP and  $N\sqrt{SWAP}$  gates are  $t_{op3} = 2\pi \times \frac{3}{2g}$  and  $t_{op4} = 2\pi \times \frac{3}{2g}$  respectively. So, the direct calculation shows that the operations times are  $t_{op3} = 7.5ns$  and  $t_{op4} = 15ns$ .

### 3.3 Implementation of NTQ-NOT gate

In this subsection, we focus on how to realize NTQ-NOT gate ( $N$  two-transmon qubit-NOT gate) with one transmon qubit simultaneously controlling  $N$  target qubits by introducing the qubit-qubit interaction. The quantum NTQ-NOT operation on two-qubit computational basis is defined through the following input-output relations:

$$\begin{aligned} U_{NOT}|0_i\rangle|0_j\rangle &= |1_i\rangle|1_j\rangle; U_{NOT}|0_i\rangle|1_j\rangle = |1_i\rangle|0_j\rangle, \\ U_{NOT}|1_i\rangle|0_j\rangle &= |0_i\rangle|1_j\rangle; U_{NOT}|1_i\rangle|1_j\rangle = |0_i\rangle|0_j\rangle. \end{aligned} \quad (22)$$

The method presented so far for implementing the NTQ-NOT gate is based on the evolutions of the subsubsection 1 (see Eq.15) where an overall phase factor  $e^{-i\eta\pi}$  is omitted. By setting  $\chi\tau = (2k + \frac{1}{2})\pi$  (with  $k$  being an integer),  $\eta = 2m + \frac{3}{2}$  (with  $m$  being an integer) and  $\gamma\tau = (2n + 1)\pi$  (with  $n$  being an integer), we can easily verify that

$$\begin{aligned} U_{NOT}(1, j)|0_1\rangle|0_j\rangle &= |1_1\rangle|1_j\rangle \\ U_{NOT}(1, j)|0_1\rangle|1_j\rangle &= |1_1\rangle|0_j\rangle \\ U_{NOT}(1, j)|1_1\rangle|0_j\rangle &= |0_1\rangle|1_j\rangle \\ U_{NOT}(1, j)|1_1\rangle|1_j\rangle &= |0_1\rangle|0_j\rangle. \end{aligned} \quad (23)$$

It's worth to point out that  $N$  two-transmon qubit-NOT operations are simultaneously performed on  $N$  qubit pairs  $(1, 2), (1, 3), \dots, (1, N + 1)$ , Each SWAP operation includes the same control qubit and a different target qubit. Then, the  $N$  two-transmon qubit-NOT gates are implemented simultaneously between one transmon qubit and  $N$  qubits. Hence, it is clear that the NTQ-NOT gate can be realised in circuit QED. Now, we give a brief discussion about quantum NTQ-NOT gate. We notice that  $\delta$  satisfies the equation  $(g/\delta_5)^2 = n + \frac{1}{2}$ , where  $n$  is an integer, when  $n = 0$ ,  $\delta$  takes maximum  $\delta_5 = \sqrt{2}g$ . Then, the operation time is  $t_{op5} = 2\pi \times \frac{3\sqrt{2}}{2g}$ . So, the direct calculation shows that the operation time required to implement the NTQ-NOT gate will be  $t_{op5} = 10.61ns$ .

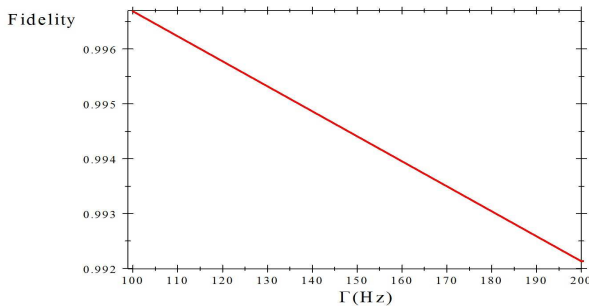


**Fig. 2:** Numerical results for fidelity of the gates operations versus the force qubit-qubit coupling  $\Gamma$ .

#### 4 Possible experimental implementation

Let us now study the fidelity of the gate operation. In order to check the validity of our proposal, we define the following fidelity to characterize the deviation of how much the output states  $|\Psi(t)\rangle$  deviate in amplitude and phase from the ideal logical gate transformation for the different input states [35]

$$F = |\langle \Psi(t) | U(t) | \Psi(0) \rangle|^2, \quad (24)$$

where  $|\Psi(t)\rangle$  is the final state of the whole system after the gate operations,  $|\Psi(0)\rangle$  is the initial state followed by an ideal phase operation and  $U(t)$  is the overall evolution operator of the system are performed in a real situation. We numerically simulate the relationship between the fidelity of the system and the force qubit-qubit coupling  $\Gamma$ . Our numerical calculation shows that a high fidelity can be achieved when  $\Gamma = 100$  Hz (see Fig. 2).

For this method to work, we discuss some issues which are relevant for future experimental implementation of our proposal. Compared with the usual charge qubit, the transmon qubit is immune to the  $1/f$  charge noise and it has much longer dephasing time as a result of the transmon qubits chosen in the system. For the sake of definiteness, let us consider the experimental parameters of the transmon qubits as  $C_g = 1aF$ ,  $C_{J0} = 300aF$ ,  $E_c = 2\pi \times 2GHz$  and  $E_J \simeq 2\pi \times 100GHz$  [15]. The transmon qubits with these parameters are available at present. Thus, the coupling three qubits with a transmission line resonator has been experimentally demonstrated [36]. Our scheme may have potential applications in multipartite entanglement. The charge fluctuations are principal only in low-frequency region and can be reduced by the echo technique [37] and by controlling the gate voltage to the degeneracy point, but an effective technique for suppressing charge fluctuations and keep the state coherent for a longer time is highly desired. So our proposal is realizable with presently available circuit QED techniques.

In a recent experiments, it was shown that the decoherence times  $T_1$  and dephasing time  $T_2$  can be made

to be on the order of  $20 - 100 \mu s$  for transmon qubits (when  $E_J/E_C = 50$ ) [38,39]. In addition, the coupling strength is  $g = 2\pi \times 200MHz$  [22,16], which is experimentally available. Furthermore, the operation time required to implement the  $Ni$ SWAP,  $N\sqrt{i}$ SWAP,  $NSWAP$ ,  $N\sqrt{S}$ WAP and  $NTQ$ -NOT gates with transmon qubits is independent of the number of target qubits  $N$ . It is clear from the above calculation that the total operation time ( $t_{op1}$ ,  $t_{op2}$ ,  $t_{op3}$ ,  $t_{op4}$  and  $t_{op5}$ ) of the quantum logic gates ( $Ni$ SWAP,  $N\sqrt{i}$ SWAP,  $NSWAP$ ,  $N\sqrt{S}$ WAP and  $NTQ$ -NOT gates) which is much shorter than the decoherence times  $T_1$  and dephasing time  $T_2$ , which satisfies our experimental requirement. Also, we note that the decoherence time of field state inside a resonator depends on the initial field state. However, the gate operation is independent of the initial state of the resonator because of the operator  $U_{gate}$  does not include the photon operator  $a$  and  $a^+$  of the circuit QED.

#### 5 Conclusion

In Summary, We have used the system in which the transmon qubits are capacitively coupled to a TLR driven by a strong microwave field. As shown above, we have presented and demonstrated a method for realizing an  $Ni$ SWAP,  $N\sqrt{i}$ SWAP,  $NSWAP$ ,  $N\sqrt{S}$ WAP and  $NTQ$ -NOT gates in circuit QED by introducing the qubit-qubit interaction. The operation time is independent of the number of qubits involved in the scheme, and the gates operations are insensitive to the initial state of the resonator. The system requires no disagreement between the qubits and the resonator. In addition, the operation time is only dependent of the detuning and the time can be controlled by adjusting the frequency between the  $|0_j\rangle$  and  $|1_j\rangle$ . However, we have calculated an evolution operator in the case of the qubit-qubit interaction. Finally, we have applied the overall evolution operator to working basis of the qubit 1 and the qubits  $j$  ( $j = 2, \dots, N+1$ ) for find the  $Ni$ SWAP,  $N\sqrt{i}$ SWAP,  $NSWAP$ ,  $N\sqrt{S}$ WAP and  $NTQ$ -NOT gates. In the our system, when we choose suitable detuning, the quantum logic gates can be realized in a time much shorter than decoherence time, and it is more immune to the  $1/f$  charge noise and have longer dephasing time as a result of the transmon qubits chosen in the system. In addition, numerical simulation of the gate operations shows that the scheme could be achieved with high fidelity under current state-of-the-art technology. Therefore, the present scheme might be realizable using the presently available techniques, and the experimental implementation of the present scheme would be a important step toward more complex quantum logic gates, serving to show the power of the transmon-qubit system for quantum information processing.

## References

- [1] R. P. Feynman, Simulating physics with computers, *International journal of theoretical physics*, 21, 467, (1982).
- [2] J. A. Smolin, G. Smith and A. Vargo. "Oversimplifying quantum factoring". *Nature*, 499, 163, (2013).
- [3] A. Farouk et al.. *Quantum computing and cryptography: an overview*, in book Series Studies in Big Data, Vol. 33, Springer, (2018).
- [4] M. A. Nielsen and I. L. Chuang. *Quantum Computation and Quantum Information*. Cambridge University Press, England, (2004).
- [5] D. Paredes-Barato and C. S. Adams. All-optical quantum information processing using Rydberg gates. *Physical review letters*, 112, 040501, (2014).
- [6] M. AbuGhanem , A. H. Homid and M. Abdel-Aty . Cavity control as a new quantum algorithms implementation treatment. *Front. Phys.* 13(1), 130303, (2018).
- [7] X. Lin, R-C. Yang, and X. Chen. Implementation of a quantum gate for two distant atoms trapped in separate cavities. *Int. J. Quantum Inform*, 13, 1550003, (2015).
- [8] J. Ferrando-Soria et al.. A modular design of molecular qubits to implement universal quantum gates. *Nat. Commun*, 7, 11377, (2016).
- [9] J. C. Garcia-Escartin and P. Chamorro-Posada. A SWAP gate for qudits. *Quantum Information Processing*, vol. 12, no. 12, pp. 3625–3631, (2013).
- [10] A. Chouikh, T. Said, K. Essammouni, M. Bennai. Implementation of universal two- and three-qubit quantum gates in a cavity QED. *Opt Quant Electron*, 48:463, (2016).
- [11] K. Eckert et al.. Quantum computing in optical microtraps based on the motional states of neutral atoms. *Phys. Rev. A*, 66, 042317, (2002).
- [12] K. Koshino, S. Ishizaka, and Y. Nakamura. Deterministic photon-photon  $\sqrt{\text{SWAP}}$  gate using a lambda system. *Physical Review A*, 82(1), 010301, (2010).
- [13] T. Wu and L. Ye. Implementing Two-Qubit SWAP Gate with SQUID Qubits in a Microwave Cavity via Adiabatic Passage Evolution. *Int J Theor Phys*, 51:1076–1081, (2012).
- [14] M. Hua, M. J. Tao, and F. G. Deng. Fast universal quantum gates on microwave photons with all-resonance operations in circuit QED. *Sci. Rep.*, 5, 9274, (2015).
- [15] C. P. Yang, Y. X. Liu, and F. Nori. Phase gate of one qubit simultaneously controlling n qubits in a cavity. *Phys. Rev. A*, 81, 062323, (2010).
- [16] G. L. Gao et al..  $1 \rightarrow N$  quantum controlled phase gate realized in a circuit QED system. *Science China Phys*, 55(8), 1422-1426, (2012).
- [17] K. H. Song, Y. J. Zhao, Z. G. Shi, S. H. Xiang, X. W. Chen. Simultaneous implementation of n SWAP gates using superconducting charge qubits coupled to a cavity. *Optics Communications*, 10, 1016, (2010).
- [18] T. Said , A. Chouikh, K. Essammouni and M. Bennai. Implementing N-quantum phase gate via circuit QED with qubit qubit interaction. *Mod. Phys. Lett. B*, 30 No. 0, 1650050, (2016).
- [19] T. Said , A. Chouikh, K. Essammouni and M. Bennai. REALIZING AN N-TWO-QUBIT QUANTUM LOGIC GATES IN A CAVITY QED WITH NEAREST QUBIT-QUBIT INTERACTION. *Quantum Information and Computation*, Vol. 16 No. 5&6, 0465–0482, (2016).
- [20] C. W. Wu et al.. Fast quantum phase gate in a small-detuning circuit QED model. *Phys Rev A*, 82, 014303, (2010).
- [21] S. H. W. van der Ploeg et al.. Controllable coupling of superconducting flux qubits. *Phys. Rev. Lett.* 98, 057004, (2007).
- [22] A. Blais et al.. Quantum-information processing with circuit quantum electrodynamics. *Phys Rev A*, 75, 032329, (2007).
- [23] D. Zueco et al.. Qubit-oscillator dynamics in the dispersive regime: Analytical theory beyond the rotating-wave approximation. *Physical Review A*, 80, 033846, (2009).
- [24] L. Ye and G.C. Guo. Scheme for implementing quantum dense coding in cavity QED. *Phys. Rev. A*, 71, 034304, (2005).
- [25] Z. J. Deng, M. Feng, and K. L. Gao, "Simple scheme for two-qubit Grover search in cavity QED". *Phys. Rev. A*, 72, 034306, (2005).
- [26] S.B. Zheng, G.C. Guo. Teleportation of atomic states within cavities in thermal states. *Phys. Rev. A*, 63, 044302, (2001).
- [27] K. Essammouni, A. Chouikh, T. Said and M. Bennai. niSWAP and NTCP gates realized in a circuit QED system. *Int. J. Geom. Methods Mod. Phys.*, 14, 1750100, (2017).
- [28] T. Said, A. Chouikh, M. Bennai. Simultaneous Implementation of NiSWAP and NSWAP gates using N + 1 qubits in a cavity or coupled to a circuit. *Journal of Experimental and Theoretical Physics*, Volume 126, Issue 5, pp 573–578, (2018).
- [29] T. Tanamoto, Y. X. Liu, X. Hu, and F. Nori. Efficient Quantum Circuits for One-Way Quantum Computing. *Phys. Rev. Lett.*, 102(10), 100501, (2009).
- [30] S. Rips and M. J. Hartmann. Quantum information processing with nanomechanical qubits. *Phys. Rev. Lett.*, 110, 120503, (2013).
- [31] M. Everitt, B. Garraway. Multiphoton resonances for all-optical quantum logic with multiple cavities. *Phys. Rev. A*, 90, 012335 (2014).
- [32] D. Deutsch, A. Barenco, A. Ekert. Universality in quantum computation. *Proc. R. Soc. London A*, 449, 669, (1995).
- [33] M. A. Nielsen, I. L. Chuang. Programmable quantum gate arrays. *Phys. Rev. Lett.*, 79, 321, (1997).
- [34] F. Vatan and C. Williams. Optimal quantum circuits for general two-qubit gates. *Phys. Rev. A*, 69, 032315, (2004).
- [35] T. Said , A. Chouikh and M. Bennai, Two-Step Scheme for Implementing N Two-Qubit Quantum Logic Gates Via Cavity QED. *Appl. Math. Inf. Sci.*, 12, No. 4, 699-704, (2018).

- [36] J. M. Fink et al.. Dressed collective qubit states and the Tavis-Cummings model in circuit QED. *Phys. Rev. Lett.*, 103, 083601, (2009).
- [37] Y. Nakamura et al.. Charge echo in a Cooper-pair box. *Phys. Rev. Lett.*, 88, 047901, (2002).
- [38] H. Paik et al.. Observation of high coherence in Josephson junction qubits measured in a three-dimensional circuit QED architecture. *Phys. Rev. Lett.*, 107, 240501, (2011).
- [39] C. Rigetti et al.. Superconducting qubit in a waveguide cavity with a coherence time approaching 0.1 ms. *Phys. Rev. B*, 86, 100506(R), (2012).



**Mohamed Bennai** is a Professor of quantum physics at Hassan II University Casablanca Morocco. He is also a visiting Professor of Theoretical Physics at Mohamed V University Rabat Morocco. He received the CEA (1990), Doctorat de 3me Cycle (1993) and the PhD (2002) from Hassan II University in Theoretical Physics. He is actually a Research Director of physics and quantum technology group at the Laboratory of Condensed Matter Physics of Ben M'sik Sciences Faculty, Casablanca, Morocco.



**Taoufik Said**

received his master degree in Systems and materials at Ibno Zohr University. He also received his PhD (2016) in the Laboratory of Physics of Condensed Matter at Ben M'sik Sciences Faculty, Casablanca, Morocco.

His research interests include modeling of quantum information processing systems, implementation of quantum algorithm in a circuit and cavity QED, realization of quantum gates in a circuit and cavity QED, quantum cryptography, information processing theory and theoretical physics.



**Abdelhaq Chouikh**

received his Graduate degree (D.E.S) in physics of materials at Casablanca An Chock Faculty of Sciences in 1996. He also received his PhD in the Laboratory of Physics of Condensed Matter at Faculty of Ben M'sik Sciences, Casablanca,

Morocco. His research interests include modeling of quantum information processing systems, implementation of quantum algorithm in a system QED, realization of quantum gates in a system QED.